A New Shape from Shading Approach for Specular Surfaces

Guohui Wang, Wei Su, and Yugui Song

School of Optoelectronic Engineering, Xi'an Technological University
Xi'an 710032, China
booler@126.com, leitin@126.com, petersong96@yahoo.com.cn

Abstract. Shape recovery is a basic problem in computer vision. Shape from shading (SFS) is an approach to get the 3D shape from a single shading image. Diffuse model is usually used to approximate the surface reflectance property. For specular surfaces, however, it is not suitable. In this paper, we propose a new SFS approach for specular surfaces. The Blinn-Phong reflectance model is applied to characterize the specular reflection property. The image irradiance equation for specular surfaces is obtained under the assumptions that the camera performs an orthographic projection and its direction is the same as the light source. Then, it is formulated as an Eikonal PDE which includes the shape of the surfaces. The viscosity solution of the resulting PDE is approximated by using the high-order Godunov fast sweeping method. Experiments are performed on both sphere and vase images and the results show the efficiency of the proposed approach.

Keywords: shape from shading, specular surfaces, Eiknoal PDE, high-order fast sweeping method.

1 Introduction

Shape recovery is a basic problem in computer vision. Shape from shading (SFS), presented by Horn [1], is an approach to get the 3D shape from one single shading image. Horn firstly derived an image irradiance equation expressing the relationship between the shape of a surface and its corresponding brightness variations. There are mainly two steps in solving SFS problem [2]. The first step is to formulate the image irradiance equation based on the certain assumption, which is the modeling of the image formation process and is determined by three factors: the camera, the light source and the reflectance property of the surface. The second step is to design a numerical algorithm to obtain a solution of the image irradiance equation, which is the shape of the given intensity image.

Since Horn's work, a large number of different SFS approaches have come out [2, 3]. Horn and Brooks [4] used the variational approach to solve the SFS problem. The shape was recovered by minimizing an energy function which consists of several constrains such as smoothness constraint and integrability constraint. To obtain a unique solution, Rouy and Tourin [5] presented a viscosity solution approach to SFS based on the Hamilton-Jacobi-Bellman equation and the viscosity solution theories.

H. Deng et al. (Eds.): AICI 2011, Part III, LNAI 7004, pp. 71–78, 2011.

Tsai and Shah [6] applied the linear approximation to the reflectance function in terms of the depth directly. Their method reconstructed the shape with a Jacobi iterative scheme. Lee and Kuo [7] proposed an iterative SFS algorithm with perspective projection. They approximated a smooth surface by the union of triangular surface patches which involved only the depth variables. The shape was reconstructed by linearizing the reflectance map and minimizing a quadratic cost functional. With the work of Rouy and Tourin [5], Kimmel and Sethian [8] presented a novel orthographic SFS algorithm. They formulated the image irradiance equation as an Eikonal PDE and computed it by using the fast marching method [9]. Yuen et al. [10] proposed a perspective SFS through extending the SFS method of Kimmel and Sethian [8]. Tankus et al. [11] derived the image irradiance equation under the perspective projection and solved it by using the iterative fast marching method. They suggested the orthographic fast marching method [8] as the initial solution, and then solved the perspective problem with an iterative method. It is well worth mentioning that Prados had made a great contribution to the SFS field [12]. They generalized the problem of orthographic and perspective SFS and associated the image irradiance equation with a Hamiltonian and approximated its viscosity solution using optimal control strategy.

Although the above work make a great deal of research, most of them concentrate on the diffuse surfaces and use Lambertian model to approximate the reflectance property. For specular surfaces, obviously, it is not suitable. Recently, Lee and Kuo [13] proposed a generalized reflectance map model, where the camera performs a perspective projection and the reflectance model is a linear combination of Lambertian and Torrance-Sparrow model [14] for the diffuse reflection and specular reflection. Ahmed and Farag [15] used Ward model [16] to express the specular surfaces. Both Torrance-Sparrow and Ward model, however, are complicated to be used in SFS problem and not easy to solve the corresponding image irradiance equation.

In this paper, we propose a new SFS approach for specular surfaces. The Blinn-Phong reflectance model [17] is applied to characterize the reflectance property of the specular reflection. The image irradiance equation for specular surfaces is obtained under the assumptions that the camera performs an orthographic projection and its direction is the same as the point light source. Then, the equation is formulated as an Eikonal PDE which includes the shape of the specular surfaces. The viscosity solution of the resulting Eikonal PDE is approximated by using the high-order Godunov fast sweeping method which is developed in our preceding work [18].

2 Image Irradiance Equation Base on the Blinn-Phong Model

With the basis that the optical axis of the camera is $z-$ axis and the image plane is $x-y$ plane, the SFS problem can be considered as that of recovering a smooth surface, z, satisfying the image irradiance equation [4]:

$$I(x,y) = R(p(x,y), q(x,y)), \tag{1}$$

where $I(x,y)$ is the image irradiance and equals to the image brightness. R is the reflectance map conducted by the reflectance model. $p \equiv z_x(x,y)$ and $q \equiv z_y(x,y)$ denote the first partial derivatives of z with respect to x and y respectively.

Assuming that the camera performs an orthographic projection, we can use the following equation to express the normal vector $\mathbf{n}$ at the point $(x, y, z(x, y))$:

$$\mathbf{n} = [p, q, -1]^T. \tag{2}$$

Figure 1 shows the reflection geometry model of a surface. $\mathbf{L}$ is the incident direction of the light source, $\mathbf{R}$ is the reflection direction, $\mathbf{V}$ is the direction of the camera, and $\mathbf{h}$ is the angular bisector of $\mathbf{L}$ and $\mathbf{V}$. θ_i, ϕ_i and θ_r, ϕ_r are the incident slant, tilt angles and the camera slant, tilt angles, respectively. δ is the angle between $\mathbf{n}$ and $\mathbf{h}$.

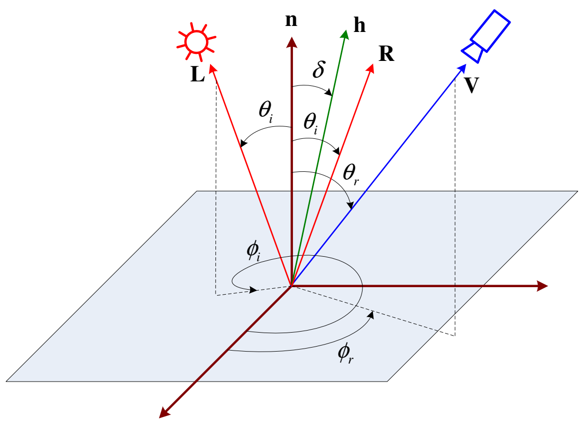

Fig. 1. Reflection geometry model

For a specular surface, Torrance and Sparrow [14] used the following equation to compute the surface reflected radiance:

$$L_s = E_0 \frac{1}{\cos\theta_r} \exp(-\frac{\delta^2}{\sigma^2}), \tag{3}$$

where E_0 is the intensity of the light source. The parameter σ is used as a measure of the surface roughness.

In order to get rid of the complicacy resulting from Torrance-Sparrow model, Phong [19] proposed a mathematically simple model to express the specular reflection:

$$L_s = E_0 (\frac{\mathbf{R}}{\| \mathbf{R} \|} \cdot \frac{\mathbf{V}}{\| \mathbf{V} \|})^N, \tag{4}$$

where N is a power which models the specular reflected light and can also be applied as a measure of shininess of the surface. Obviously, it is not convenient to compute the surface radiance in terms of $(\mathbf{R} \cdot \mathbf{V})$.

For convenience, Blinn [17] presented another mathematically simple model (5) by substituting $(\mathbf{n}\cdot\mathbf{h})$ into $(\mathbf{R}\cdot\mathbf{V})$ of Eq. (4).

$$L_s = E_0\left(\frac{\mathbf{n}}{\|\mathbf{n}\|}\cdot\frac{\mathbf{h}}{\|\mathbf{h}\|}\right)^N = E_0(\cos\delta)^N. \tag{5}$$

Assuming that the direction of the light source is the same as the direction of the camera, we have $\theta_i=\theta_r$, $\phi_r=\phi_i$. As a result, Eq. (5) has been transformed into

$$L_s = E_0(\cos\theta_i)^N. \tag{6}$$

If we define that the direction vectors of the light source and the camera are also $[0,0,-1]^T$ and because θ_i is the angle between $\mathbf{n}$ and $\mathbf{L}$, in this case, we have

$$\cos\theta_i = \frac{\mathbf{n}}{\|\mathbf{n}\|}\cdot\frac{\mathbf{L}}{\|\mathbf{L}\|} = \frac{1}{\sqrt{1+p^2+q^2}} = \frac{1}{\sqrt{1+\|\nabla z\|^2}}. \tag{7}$$

The substitution of Eq. (7) into Eq. (6), the reflectance map and the image irradiance equation conducted by the Blinn-Phong model are expressed as

$$R(p,q) = \left(\frac{1}{\sqrt{1+\|\nabla z\|^2}}\right)^N = I(x,y). \tag{8}$$

The Eq. (8) is also derived as

$$\|\nabla z(x,y)\| = \sqrt{I(x,y)^{-2/N}-1} = F(x,y). \tag{9}$$

Now the SFS problem (8) can be derived as the following standard Eikonal PDE:

$$\begin{cases} \|\nabla z(x,y)\| = F(x,y) & \forall x\in\Omega \\ z(x,y)=\varphi(x,y) & \forall x\in\partial\Omega \end{cases}, \tag{10}$$

where Ω is the image domain and $\varphi(\mathbf{x})$ is a real continuous function defined on $\partial\Omega$.

3 A Numerical Algorithm to Approximate the Solution of the Resulting Eikonal PDE

In order to approximate the viscosity solution of the resulting Eikonal PDE (10), we use the numerical algorithm developed in our preceding work [18], which is the high-order Godunov fast sweeping method [20].

Consider a uniform discretization $\{(x_i,y_j)=(ih,\ jh),\ i=1,2,\cdots,m,\ j=1,2,\cdots,n\}$ of the domain Ω. By definition, $Z_{i,j}\equiv Z(x_i,y_j)$. A high-order Godunov upwind difference scheme is used to discretize the Eikonal PDE (10):

$$\left\{\max\left[\frac{z_{i,j}^{new}-z_1}{h},0\right]\right\}^2 + \left\{\max\left[\frac{z_{i,j}^{new}-z_2}{h},0\right]\right\}^2 = F_{i,j}^2, \tag{11}$$

where

$$z_1 = \min[(z_{i,j}^{old} + hp_{i,j}^{+}),(z_{i,j}^{old} - hp_{i,j}^{-})\ ],$$
$$z_2 = \min[(z_{i,j}^{old} + hq_{i,j}^{+}),(z_{i,j}^{old} - hq_{i,j}^{-})\ ], \tag{12}$$

with

$$p_{i,j}^{+} = (1-\alpha_+)\left(\frac{z_{i+1,j} - z_{i-1,j}}{2h}\right) + \alpha_+\left(\frac{-z_{i+2,j} + 4z_{i+1,j} - 3z_{i,j}}{2h}\right),$$
$$p_{i,j}^{-} = (1-\alpha_-)\left(\frac{z_{i+1,j} - z_{i-1,j}}{2h}\right) + \alpha_-\left(\frac{3z_{i,j} - 4z_{i-1,j} + z_{i-2,j}}{2h}\right), \tag{13}$$

where

$$\alpha_+ = \frac{1}{1+2\beta_+^2},\ \beta_+ = \frac{\varepsilon + (z_{i+2,j} - 2z_{i+1,j} + z_{i,j})^2}{\varepsilon + (z_{i+1,j} - 2z_{i,j} + z_{i-1,j})^2},$$
$$\alpha_- = \frac{1}{1+2\beta_-^2},\ \beta_- = \frac{\varepsilon + (z_{i,j} - 2z_{i-1,j} + z_{i-2,j})^2}{\varepsilon + (z_{i+1,j} - 2z_{i,j} + z_{i-1,j})^2}. \tag{14}$$

Here, ε is a small constant to prevent the denominator from being zero. Similarly, q^- and q^+ are defined.

Now the viscosity solution of the PDE (10) is:

$$z_{i,j}^{new} = \begin{cases} \dfrac{z_1 + z_2 + \sqrt{2h^2F_{i,j}^2 - (z_1 - z_2)^2}}{2} & |z_1 - z_2| < hF_{i,j} \\ \min[z_1, z_2] + hF_{i,j} & |z_1 - z_2| \geq hF_{i,j} \end{cases}. \tag{15}$$

The algorithm can be summarized as follows:

1) *Initialization:* Set the grid points on the boundary $\partial\Omega$ to be exact values, i.e., $z_{i,j}^{0} = \varphi_{i,j}$, which are fixed during the iterations. The solution from the first-order Godunov fast sweeping scheme is used as the initial values at all other grid points.
2) *Alternating Sweepings:* At iteration $k+1$, we compute $z_{i,j}^{new}$ according to the update formula (15) by Gauss-Seidel iterations with four alternating direction sweepings:

- From upper left to lower right, i.e., $i = 1:m,\ j = 1:n$;
- From lower left to upper right, i.e., $i = m:1,\ j = 1:n$;
- From lower right upper to left, i.e., $i = m:1,\ j = n:1$;
- From upper right to lower left, i.e., $i = 1:m,\ j = n:1$.

3) *Convergence Test:* If $\left\| z^{k+1} - z^k \right\|_{L^1} \le \mu$, where μ is a given stopping criterion, the algorithm converges and stops; otherwise returns to 2). Here, we take $\mu = 10^{-3}$.

4 Experimental Results

4.1 Experimental Results on Sphere Image

In these experiments, we employ a synthetic sphere image which is generated by the formula:

$$z(x, y) = \sqrt{R^2 - x^2 - y^2}, \tag{16}$$

where $(x, y) \in [-49, 50] \times [-49, 50]$ and $R = 40$ is the radius.

The ground truth of the vase and the synthetic image generated by the Eq. (8) are shown in Fig. 2(a) and Fig. 2(b), respectively. The parameter K is set as 5. The reconstructed surface using the presented algorithm is shown in Fig. 2(c), while the error surface with the ground truth is shown in Fig. 2(d). The algorithm stopped after 95 iterations. The mean absolute error (MAE) and the root mean square error (RMSE) are 1.2724 pixels and 1.3637 pixels, respectively.

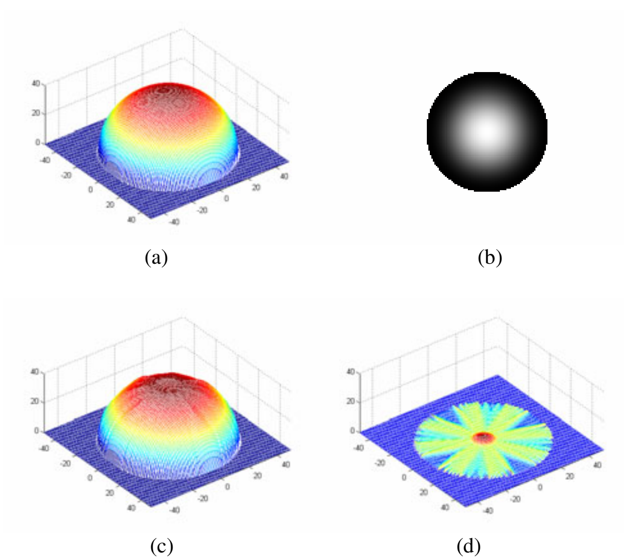

Fig. 2. Experimental results for the sphere

4.2 Experimental Results on Vase Image

In these experiments, we employ a synthetic sphere image which is generated by the formula:

$$z(x, y) = \sqrt{R^2 - x^2 - y^2}, \tag{17}$$

where $f(x) = 0.15 - 0.025(2x+1)(3x+2)^2(2x-1)^2(6x-1)$ and $(x, y) \in [-0.5, 0.5] \times [-0.5, 0.5]$. We map the x and y ranges to $[-49, 50]$ and scale $z(x, y)$ by a factor of 100. This yields a maximum depth value of approximately 28.55.

The ground truth of the vase and the synthetic image generated by the Eq. (8) are shown in Fig. 3(a) and Fig. 3(b), respectively. The parameter K is also set as 5. The reconstructed surface using the presented approach is shown in Fig. 3(c), while the error surface with the ground truth is shown in Fig. 3(d). The algorithm stopped after 126 iterations. The MAE and RMSE are 1.0057 pixels and 1.1157 pixels, respectively.

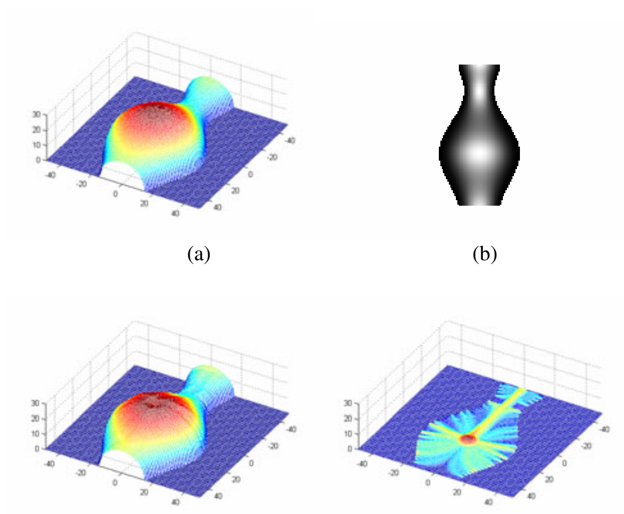

(a) (b)

(c) (d)

Fig. 3. Experimental results for the vase

5 Conclusion

This paper proposes a new SFS approach for specular surfaces. We apply the Blinn-Phong reflectance model to characterize the reflectance property of the specular reflection. The image irradiance equation for specular surfaces is obtained under the assumptions that the camera performs an orthographic projection and its direction is the same as the point light source. Then, the equation is formulated as an Eikonal PDE which includes the shape of the surfaces, and we approximate the solution of the resulting Eikonal PDE by using the high-order Godunov fast sweeping method. Experiments are conducted on both sphere and vase images and the results show that the proposed approach is effective and accurate.

Acknowledgments. This work is supported by the program of The Project Supported by Natural Science Basic Research Plan in Shaanxi Province of China (Program No. 2011JQ8004). At the same time, this work is supported by the Scientific Research Program Funded by Shaanxi Provincial Education Department (Program No. 11JK0996) and is also supported by the Program for Innovative Science and Research Team of Xi'an Technological University.

References

1. Horn, B.K.P., Brooks, M.J.: Shape from Shading. MIT Press, Cambridge (1989)
2. Zhang, R., Tsai, P.-S., Cryer, J.E., Shah, M.: Shape from Shading: A Survey. IEEE Trans. Pattern Anal. Mach. Intell. 21, 690–706 (1999)
3. Durou, J.-D., Falcone, M., Sagona, M.: Numerical Methods for Shape-from-shading: A New Survey with Benchmarks. Comput. Vis. Image Underst. 109, 22–43 (2008)
4. Horn, B.K.P., Brooks, M.J.: The Variational Approach to Shape From Shading. Comput. Vis. Graph. Image Process. 33, 174–208 (1986)
5. Rouy, E., Tourin, A.: A Viscosity Solutions Approach to Shape-from-shading. SIAM J. Numer. Anal. 29, 867–884 (1992)
6. Tsai, P.-S., Shah, M.: Shape from Shading Using Linear Approximation. Image Vis. Comput. 12, 487–498 (1994)
7. Lee, K.M., Kuo, C.-C.J.: Shape from Shading with Perspective Projection. Comput. Vis. Graph. Image Process. 59, 202–212 (1994)
8. Kimmel, R., Sethian, J.A.: Optimal Algorithm for Shape from Shading and Path Planning. J. Math. Imaging Vision 14, 237–244 (2001)
9. Sethian, J.A.: Fast Marching Methods. SIAM Rev. 41, 199–235 (1999)
10. Yuen, S.Y., Tsui, Y.Y., Leung, Y.W., Chen, R.M.M.: Fast Marching Method for Shape from Shading under Perspective Projection. In: The 2nd IASTED International Conference on Visualization, Imaging and Image Processing, pp. 584–589. Malaga, Spain (2002)
11. Tankus, A., Sochen, N., Yeshurun, Y.: Shape-from-Shading Under Perspective Projection. Int. J. Comput. Vis. 63, 21–43 (2005)
12. Prados, E., Faugeras, O.: A generic and provably convergent Shape-From-Shading Method for Orthographic and Pinhole Cameras. Int. J. Comput. Vis. 65, 97–125 (2005)
13. Lee, K.M., Kuo, C.-C.J.: Shape from Shading with a Generalized Reflectance Map Model. Comput. Vis. Image Underst. 67, 143–160 (1997)
14. Torrance, K.E., Sparrow, E.M.: Theory for Off-Specular Reflection From Roughened Surfaces. J. Opt. Soc. Am. 57, 1105–1114 (1967)
15. Ahmed, A.H., Farag, A.A.: Shape from Shading for Hybrid Surfaces. In: The 14th IEEE International Conference on Image Processing, vol. II, pp. 525–528. IEEE, San Antonio (2007)
16. Ward, G.J.: Measuring and modeling anisotropic reflection. ACM SIGGRAPH Comput. Graph. 26, 265–272 (1992)
17. Blinn, J.F.: Models of light reflection for computer synthesized pictures. ACM SIGGRAPH Comput. Graph. 11, 192–198 (1977)
18. Wang, G., Liu, S., Han, J., Zhang, X.: A Novel Shape from Shading Algorithm for Non-Lambertian Surfaces. In: The 3rd International Conference on Measuring Technology and Mechatronics Automation, vol. 1, pp. 222–225. IEEE, Shanghai (2011)
19. Phong, B.T.: Illumination for computer generated pictures. Comm. ACM 18, 311–317 (1975)
20. Zhang, Y.-T., Zhao, H.-K., Qian, J.: High Order Fast Sweeping Methods for Static Hamilton-Jacobi Equations. J. Sci. Comput. 29, 25–56 (2006)